

SGV 3.0 - a fast detector simulation

Mikael Berggren

DESY

Notkestraße 85, D-22607 Hamburg -Germany

The need for fast simulation programs is emphasised, both in terms of the need for “rapid response” to new results - in particular from the LHC - and new theoretical ideas, and in terms of how to cope with multi-billion simulated event samples. The latter would arise both from the need to be able to simulate significantly more events than expected in the real data, also for high cross-section processes, and the need to scan multi-parameter theories.

The *Simulation à Grande Vitesse*, SGV, is presented, and is shown to be able to address these issues. The tracking performance of SGV is shown to reproduce very closely that of the full simulation and reconstruction of the ILD concept. Preliminary results on how to also closely emulate the calorimetric performance from full simulation is presented. The procedure is parametric, with no need to simulate the detailed shower development, and promises to be many orders of magnitude faster than such approaches. Contrary to what is often the case with fast simulation programs, the procedure gives a somewhat *pessimistic* result, compared to the full simulation and reconstruction.

1 Introduction

The latest years of development has brought forward very performant and complete full simulation packages, both in SiD and ILD [1, 2]. One might then wonder why there still is any need for fast simulation of the ILC or CLIC detectors.

One answer to this was given during this conference by R. Heuer, when he pointed out that “*We need to update the physics case (for the LC) continuously*”. This means that not only does one need detailed simulation of a few bench-mark reactions - to validate the detector concepts - but also to simulate a large variety of processes, possibly from newly conceived models, or models that recently have been revised in light of observations at the LHC. To this can be added that the studies leading to the LOI [1, 2] showed that, as far as physics results were concerned, fast and full simulation studies gave close to identical results. To fulfil the needs for fast and precise physics results, such fast simulation programs need to be light-weight, to be able to run without the need of large computer resources, with a low threshold for non-experts to start using it, but most of all they need to be truly fast.

There are two cases where the speed of the simulation is of utmost importance: High cross-section background process, and multi-parameter theory scans.

1.1 Examples: $\gamma\gamma$ cross-sections and SUSY scans

At $\sqrt{s} = 500$ GeV, PYTHIA [3] estimates the total cross-section for $e^+e^- \rightarrow \gamma\gamma e^+e^- \rightarrow q\bar{q}e^+e^-$ at $E_{CMS} = 500$ GeV to be 35 000 pb. Therefore, 17.5×10^9 such events would have been produced after taking 500 fb^{-1} of data, which each ILC experiment expects to have collected in the first four years of running. A typical time to generate such events is 10 ms. A fast detector simulation would aim at not requiring more than that for the detector simulation. This leads to a total time of 3.5×10^8 s, equal to about 10 years, to generate 500 fb^{-1} of $\gamma\gamma$ events. Already with only a handful of CPU’s, such a sample could be simulated

in a few months, and with typical resource of a batch-farm (several hundred cores), not more than a few days would be needed. On the other hand, full simulation and reconstruction takes several minutes per event, ie. more than three orders of magnitude more, and would require many thousand CPU-years. Even with full-blown grid-processing, such a program would take years, possibly longer than it would take to collect the real data. It should also be noted that these numbers apply for the modest requirement that the simulated sample is the same size as the real data. This is arguably far from being sufficient: with such a small sample, the simulation statistical error might be the dominating systematic error of the measured quantities. Probably one would require as an absolute minimum that the simulated sample is five times larger than the data sample; this was the case at LEP.

An other example where very large samples need to be simulated is scanning SUSY parameter-space. MSUGRA can serve as a simple example: In this model, there are four continuously varying theory parameters and the sign of a fifth one. If one wants to scan each of the continuous parameters in 20 steps, and simulate 5000 events per point^a, about 2×10^9 events need to be simulated. Such events are slower to generate and simulate than $\gamma\gamma$ events, so also in this case CPU millennia would be needed to do full simulation.

2 The SGV fast simulation

Fast detector simulations exist of different types, with different levels of sophistication. For any approach, the aim is that the detector-simulation time of one event should be of the same order as the time to generate an event by an efficient event generator, such as PYTHIA6. One can make a simple smearing of the generated four-vectors with some global assumed detector properties. A somewhat more elaborate scheme is the parametric simulation, where measurements are parametrised with respect to particle energy and angle. SIMDET, the fast simulation program used for the TESLA TDR physics studies falls in this category [4]. Finally, one can construct covariance matrix machines, where the full covariance matrix is constructed from the generated particles and the detector layout. In this category one finds eg. LiCToy [5] and SGV - *La Simulation à Grande Vitesse*.

SGV was originally developed in the early nineties as a tool to evaluate the proposed upgrade of the DELPHI detector in view of the new conditions expected due to the transition from LEP I to LEP II [6]. It evolved into a valuable tool for new physics searches in DELPHI, both for signal and background simulation [7]. It has subsequently been used for physics and detector studies for TESLA, LDC and ILD [1, 4, 8, 9].

Over the last year, the well-tested SGV2 series (written in Fortran77) have been rewritten and re-organised into an SVN-managed Fortran95 package. Most of the previous versions dependence on CERNLIB has been removed^b, the installation procedure has been re-written, and new features have been added, and more are planned. SGV has been tested to work on both 32 and 64 bit architectures out-of-the-box, and it was verified that the transformation from Fortran77 to Fortran95 did not deteriorate the speed. In fact, the Fortran95 version was found to be faster (by 15%) than the Fortran77 version.

^aA modest requirement: in eg. the MSUGRA point sps1a' almost 1 million SUSY events are expected for 500 fb^{-1} .

^bWork will be done to further reduce CERNLIB dependence. This will inevitably be at a the cost of backward compatibility on steering files, as the usage of the FFREAD package would in that case be replaced by using Fortran namelists, which has the same functionality, but different syntax. HBOOK dependence will remain in the foreseeable future - but only for user convenience : SGV itself doesn't need it.

Among the features of SGV are:

- Both PYTHIA [3] and Whizard [10] are internally callable.
- Alternatively, input can be read from PYJETS or StdHep [11].
- The same formats can be used to output the generated event.
- A `samples` subdirectory with steering and code for eg. scanning single particles, create an HBOOK ntuple with “all” information, which can be converted to ROOT using the `h2root` tool. There is also code to output the simulated event in LCIO DST-format [12].

Features that are foreseen to be added to SGV in the near future are:

- Development on calorimeters, which will be detailed in Chapter 3.
- Including a filter-mode, which would allow to simulate large samples with varying detail as needed for a specific analysis. One would generate the event inside SGV and subsequently run the SGV detector simulation and analysis. From the result of the analysis, the fate of the event can be determined, from completely discarding it, over filling control-histograms, writing it to an ntuple, to LCIO, or to request full simulation, by outputting the generated event in StdHep format.

To install SGV, one should first execute (preferably in a new, empty directory):

```
svn export https://svnsrv.desy.de/public/sgv/tags/SGV-3.0rc1/ SGV-3.0rc1/
```

followed by

```
cd SGV-3.0rc1 ; bash install
```

These two commands will take about a minute to complete. The main documentation is in the README file in the top-directory, and for various specific tasks and examples, the README:s in the `samples` sub-directory and it’s sub-directories. This allows to get various external programs installed, if they are not already available on the system. This includes StdHep, CERNLIB (in native 64bit), Whizard (both basic and ILC-tuned versions), and the LCIO-DST writer.

2.1 Simulation of the tracking detectors

As stated above, SGV is a machine to calculate covariance matrices. The procedure used is as follows [13]: The track-helix is followed through the detector, to find what layers are hit by the particle, as illustrated in Figure 1, showing the $R\phi$ projection of a quadrant of the ILD detector, as it is described in SGV. The outward tracking continues until the intersection of the start of the out-most calorimeter is reached. The helix is locally described either by barrel coordinates, or forward coordinates, depending of the nature of the intersected surface. In the forward-barrel overlap region, it can possibly switch between these descriptions several times along it’s trajectory.

From the list of intersected surfaces, the covariance matrix at the perigee is calculated: The helix is followed from the outside, starting at the outer-most tracking-detector surface. At each recorded intersection, the measurements the surface contributes are added in quadrature to the relevant elements of the covariance matrix. The matrix is then inverted, to obtain the weight matrix. The effect of multiple-scattering [14] at the surface is added to the relevant elements of this matrix. The matrix is then once again inverted, and translated

along the helix (in five-dimensional helix-space) to the next intersected surface, and the procedure is repeated. This continues until the mathematical surface representing the point of closest approach is reached. As each track is followed through the detector, the information on hit-pattern is automatically obtained, and is made accessible to later analysis.

It can be noted that this method can be described in mathematical terms as a realisation of a Kalman filter [15,16], and often in particle physics “Billoir track-fit” and “Kalman filter” are treated as synonyms. In SGV, the formalism of Kalman filters is not used, rather all matrix operations, including the inversions, are worked out in element-form in the code, to avoid having to call general-purpose numerical methods, which possibly are inefficient for the problem at hand and might impede on the performance of the optimisation done by the compiler.

The perigee parameters are then smeared according to the calculated covariance matrix. This uses the method of doing a Cholesky decomposition [17] of the matrix, and then multiplying the lower-triangular component (L) with a vector (u) filled with uncorrelated random variables. The product vector $v = Lu$ will contain random numbers with correlations between them that are indeed those of the calculated covariance matrix. Figure 2 shows a few examples of the excellent agreement between the SGV result and that obtained by the full simulation and reconstruction for the same detector configuration.

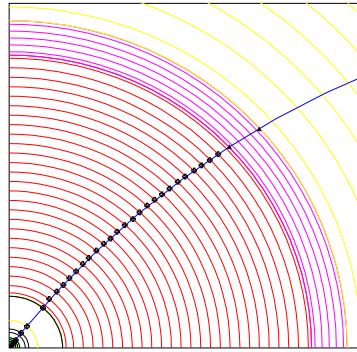


Figure 1: A graphical rendering of the method described in the text.

2.2 Simulation of calorimeters

To simulate calorimeters, the charged or neutral particle is extrapolated to the intersections with the various calorimeters. A decision is made on how the detectors will act. It can be concluded that the particles should be detected as a minimum ionising one, or that it should initiate an electromagnetic shower, or a hadronic shower, or that it is below the detectability threshold. According to the chosen process, the detector response is simulated from parameters, given in the geometry description input-file. As a final (non-obligatory) step, showers can be merged if they are sufficiently close. The code that tracks the particles to the intersections is separated from the code simulating the response, so by replacing the latter (at compile-time) with a user-supplied routine, any other shower-simulation can be used. It should be kept in mind, however, that any more sophisticated algorithm probably is orders of magnitude slower, and would denigrate the main benefit of a fast simulation. A step towards increasing the realism is to simulate confusion between calorimetric clusters. The procedure to emulate the full reconstruction in this respect is described below, in Section 3.

2.3 Additional simulation features

In addition to the above core-functionality of SGV, the program also allows for the simulation of electromagnetic interactions (pair-creation and bremsstrahlung) in the detector material,

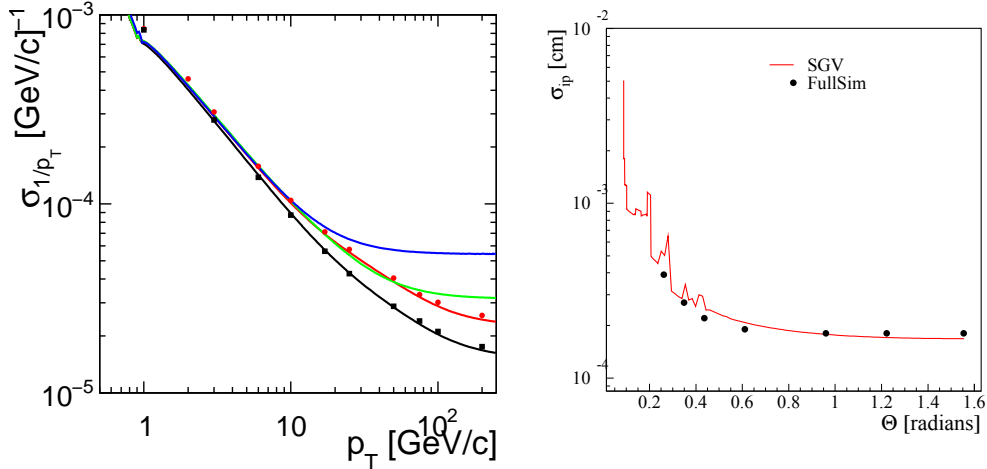


Figure 2: Left plot: The momentum error σ_{1/p_T} vs. p_T , for a number of different detector configurations. Right plot: The impact-parameter error σ_{ip} vs. p_T . The lines show the SGV result, and the dots show the full simulation and reconstruction result.

and has a well-defined scheme on how to plug in code simulating particle identification, track-finding efficiencies (both on the whole-track and hit level), and the presence of scintillators or taggers (ie. detector-elements that only measure the presence, within the acceptance of the element, of particles above a threshold.)

3 Calorimeter simulation tuning

The basic issues of a fast simulation of calorimeters - the random error on the detected energy, on the shower position, and on it's shape - are included by default in SGV. However, there are also association errors: Clusters might merge, might split, or might get wrongly associated to tracks. Since the measurement by the tracking system - if it is available - is always preferred to the calorimetric measurement, association errors entails errors on the total reconstructed energy: On one hand, if a (part of) a neutral cluster gets associated to a charged track, energy is lost, on the other hand, if a (part of) a charged cluster is *not* associated to any track, energy is double-counted. Other errors, eg. split neutral clusters, charged cluster associated with wrong track and so on, are of less importance, since they do not give rise to an error on the total event energy or momentum.

In SGV, information is already available about where the particle hits the calorimeters. The program contains procedures to generate errors on energy, position and shower-axes from geometry file input parameters, to merge clusters based on generated shower positions and axes to accommodate errors in the association between clusters and tracks. All these procedures can be controlled by the SGV geometry and steering-files. Therefore, the next step to further increase the realism of the simulation is to treat the association errors.

To study association errors, a sample was selected from the LOI mass-production - 8 thousand $e^+e^- \rightarrow udsc$ fully simulated and reconstructed events. The particles recon-

structured using the particle-flow algorithm Pandora [18] were compared to the true particles. To be able to compare only the effects of the treatment of calorimeters, not differences in the treatment of interactions and measurement in the tracking volume, the true particles and reconstructed tracks were read from the full simulation DST. The calorimeter hits were also read from there, and were used to create true clusters, ie. clusters made exclusively by calorimeter hits created by a certain true particle. The study concentrated on the most important issues, ie. double-counting and energy loss, while neutral-neutral or charged-charged merging was not considered, nor was multiple splitting/merging. Among the observables available in fast simulation, the most relevant ones were then identified. This included the cluster energy, the distance at the calorimeter face to nearest true particle of “the other type” (ie. neutral-to-charged or charged-to-neutral), whether the particle was a hadron or not, and whether it would be detected by the barrel or end-cap calorimeters. The confusion was then broken down into sub-processes and was found to be possible to factorise as:

1. The probability that a cluster would split: The splitting probability.
2. In the case the cluster did split: the probability to split off/merge the *entire* cluster: The complete-split probability.
3. If the case cluster did split, but not completely: the form of the p.d.f. of the fraction split off: The split-fraction.

One could observe that

1. The splitting probability depends on the isolation - strongly for energy loss, slightly for double-counting - but can be treated in two energy bins with no energy dependence in the bin, as can be seen in Figure 3. There was also a %5 over-all dependence on whether the particle was observed in the barrel or end-cap.

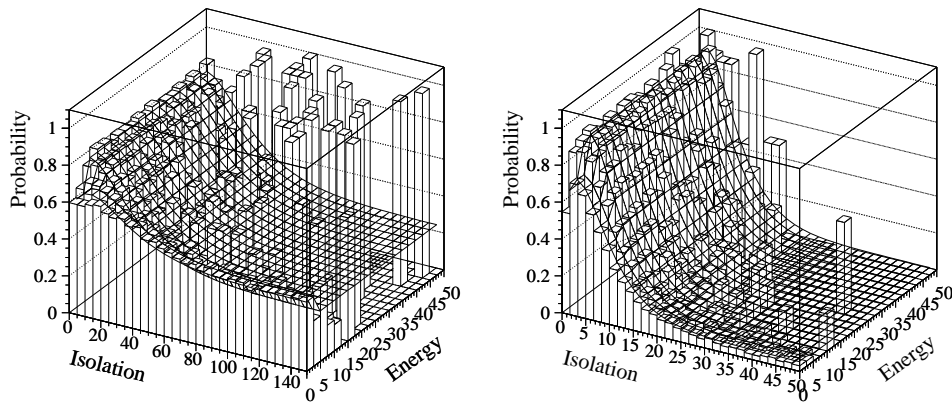


Figure 3: The probability to split clusters versus energy and isolation. The left plot shows the situation for charged hadrons (double-counting), while the right plots shows the situation for photons (energy loss). The histograms shows the observed performance of Pandora, while the mesh is the fit.

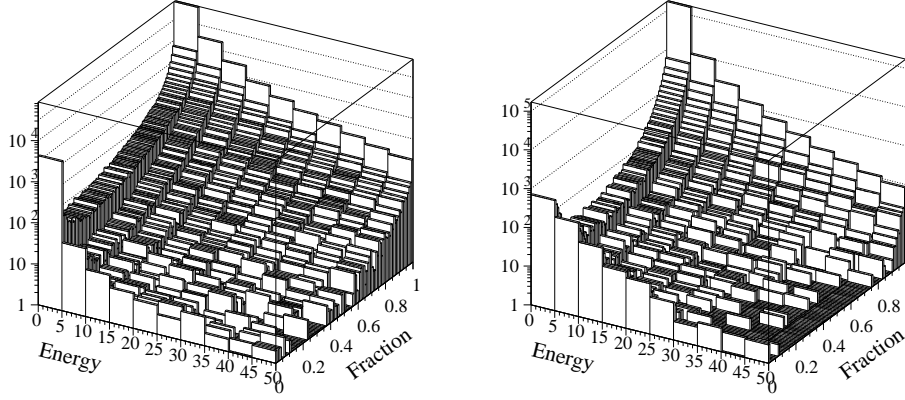


Figure 4: Fraction of cluster-energy correctly attributed versus cluster energy. The left plot shows the situation for charged hadrons (double-counting), while the right plots shows the situation for photons (energy loss).

2. The complete-split probability depends only on the particle's energy, as can be seen in Figure 4, by looking at the fraction = 0 bin.
3. The split-fraction depends on both energy and isolation, see Figure 5. However, it was also found that the energy and distance dependence of the shape could be described by how the average fraction depended on these variables. This dependence is shown in Figure 6

All cases (electromagnetic or hadronic cluster - double-counting or energy loss - Barrel or end-cap) can be described by the same functional shapes, only the parameter-values differ

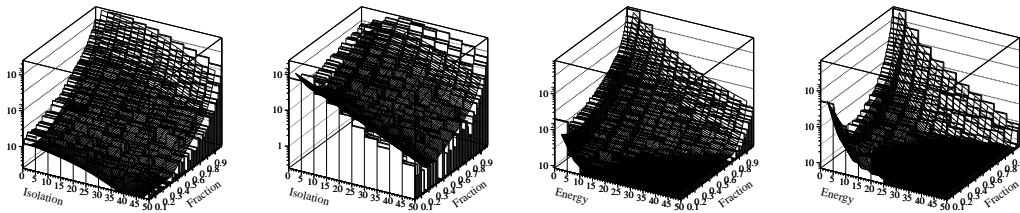


Figure 5: Fraction of cluster-energy correctly attributed versus either isolation (the two plots to the left) or cluster energy (the two plots to the right). The plot to the left in each case shows the situation for charged hadrons (double-counting), while the one to the right shows the situation for photons (energy loss). The histograms shows the observed performance of Pandora, while the mesh is the final fit. The bins with fraction 0 (complete split) and 1 (no split) are suppressed.

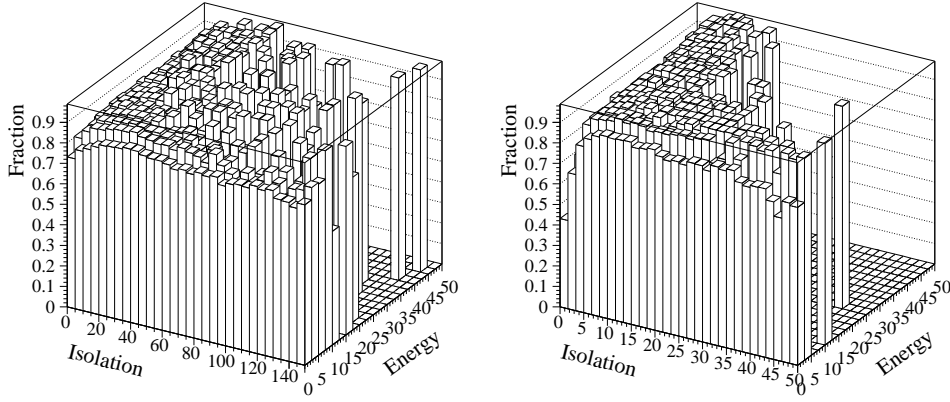


Figure 6: The average of the correctly assigned fraction of the cluster energy versus isolation and cluster energy. Right: the situation for charged hadrons (double-counting). Left: the situation for photons (energy loss).

between the cases. The fitted functions could be conveniently chosen as combinations of exponentials and lines. A total of $28 \text{ parameters} \times 4 \text{ cases (em/had} \times \text{double-counting/loss)}$ are found to be needed.

When analysing the fully simulated and reconstructed sample, the three fitted functions could be used to simulate double-counting or energy loss for each true particle. This para-

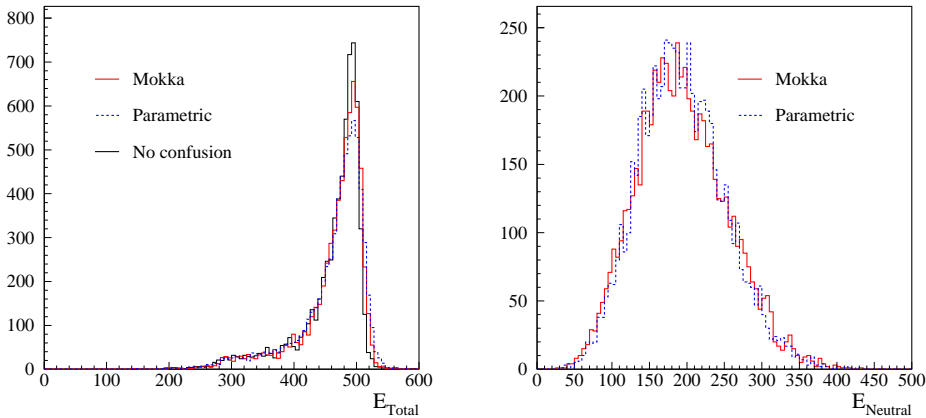


Figure 7: Total seen energy (left), and total seen neutral energy (right). The red line shows the full reconstruction, the blue dashed curve, the parametric smearing of confusion, and the black solid line the case with no confusion.

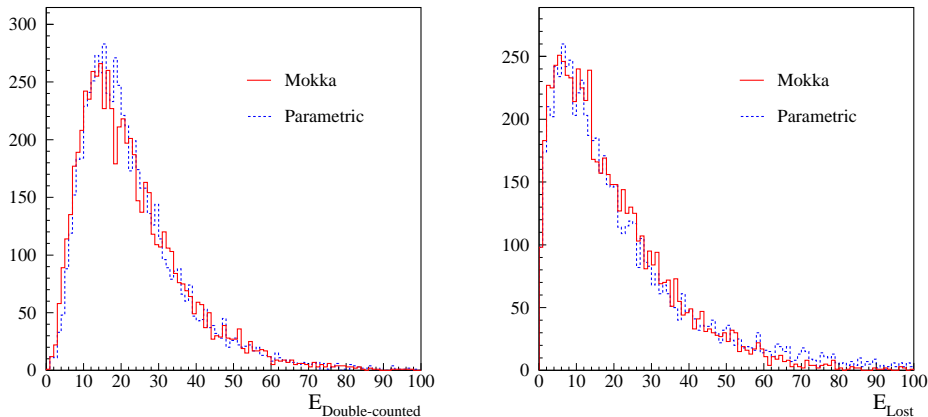


Figure 8: Double-counted energy (left) and lost energy (right). The curves have the same meaning as in Fig 7.

metrically simulated detector-response could then be compared with the results of the full reconstruction. A number of global parameters were adjusted to get the best possible agreement. These parameters include the ratio between cluster-energy and track momentum for charged particles and the overall probability to split clusters. In Figure 7, the total seen energy and the total neutral energy distributions are shown, and Figure 8 shows the lost and double-counted energy distributions. One can observe that a quite good agreement was obtained both for the amount of the two contributors to the confusion (double-counting and energy loss) and for the global event variables. By studying the width of the three curves in the total energy figure, it can be noted that the parametric confusion term is somewhat larger than what the full reconstruction yields. Therefore, the SGV with this tuning applied would be somewhat on the pessimistic side, which is un-usual for fast simulation programs.

4 Conclusions

We have pointed out need for fast simulation programs, both in order to be able to quickly evaluate new theories confronted with a realistic experimental situation, and to cope with cases where multi-billion event samples would be requires *viz.* large cross-sections ($\gamma\gamma$), or large parameter-spaces in new physics scenarios. The SGV program was presented, and was shown to fulfil the requirements emerging from these considerations, both in terms of physics and of computing performance. We presented the tracking performance of SGV and found it to be close to identical to what the full simulation and reconstruction of the ILD detector yields. In addition, the way to parametrically incorporate the effects of confusion between calorimetric clusters was presented. It was shown that a modest number of parameters were needed to get a result comparable to the result of full shower development programs. The procedure was in fact such that the fast simulation result falls on the somewhat pessimistic side. The shower-parametrisation is still work in progress, and would need future validation on a larger set of physics channels.

5 Acknowledgements

The author would like to thank P. Billoir for providing the core code of the covariance-machine, and F. James for pointing to the method of Cholesky decomposition. B. Jeffery provided useful help for the LCIO interface. M. Chera and L. Dai contributed to the analysis of shower-shapes. A. de Angelis, C. de la Vassière and M. A. do Vale contributed with various routines, and the comments from K. Hultqvist, P. Luzniak and V. Adler were very helpful. Thanks is also due to F. Richard, who initiated the project. The support of the Deutsche Forschungsgemeinschaft through the Sonderforschungsbereich 676 (grant SFB 676/2-2010) is acknowledged.

6 Bibliography

References

- [1] ILD concept group, *Letter of Intent*, arXiv:1006.3396v1 (2010).
- [2] H. Aihara, P. Burrows, M. Oreglia (editors), *SiD Letter of Intent*, arXiv:0911.0006v1 (2009).
- [3] T. Sjöstrand, S. Mrenna, P. Z. Skands, *JHEP* **0605**,026 (2006).
- [4] R.-D. Heuer *et al.*, *TESLA TDR Part III*, arXiv:hep-ph/0106315 (2001).
- [5] M. Regler, M. Valentan, R. Frühwirth, *LiCToy 2.0*, HEPHY-PUB-863/08.(2008).
- [6] P. Abreu *et al.*, *Proposal for the upgrade of DELPHI in the forward region*, CERN-LEPC-92-11, LEPC-G-4, (1992)
- [7] J. Abdallah, *et al.*, (DELPHI collaboration), *Eur.Phys.J.* **C31**,421 (2003).
- [8] S. Hillert *et al.*, in “Proceedings of LCWS 2007”, arXiv:0708.2622v1 (2007).
- [9] M. Berggren, F. Richard, Z. Zhang , arXiv:hep-ph/0510088 (2005);
M. Berggren, arXiv:hep-ph/0508247 (2005);
P. Bambade, M. Berggren, F. Richard, Z. Zhang, arXiv:hep-ph/0406010 (2004);
M. Berggren, R. Keranen, H. Nowak, A. Sopczak, arXiv:hep-ph/9911345 (1999);
M. Berggren, R. Keranen, A. Sopczak, arXiv:hep-ph/9911344 (1999).
- [10] W. Kilian, T. Ohl, J. Reuter, *Eur.Phys.J.* **C71**,1742 (2011).
- [11] L. Garren, *StdHep 5.06.01*, <http://cepa.fnal.gov/psm/stdhep/> (2006).
- [12] F. Gaede, T. Behnke, N. Graf, T. Johnson , arXiv:physics/0306114v1 (2003).
- [13] P. Billoir, *Nucl.Instrum.Meth.* **A225**, 352 (1984).
- [14] G.R. Lynch, O.I. Dahl, *Nucl.Instrum.Meth.* **B58**,6 (1991).
- [15] R.E Kalman, *Trans. ASME - J, of Basic Eng.* **82D**, 35 (1960).
- [16] P. Billoir, *Comput.Phys.Commun.* **57**,390 (1989).
- [17] CERNLIB routine TRCHLU (F112).
- [18] M.A. Thomson, *Nucl.Instrum.Meth.* **A611**,25 (2009).